Feasibility of simultaneous CO2 storage and CH4 production from natural gas hydrate using mixtures of CO2 and N2

BJØRN KVAMME
Department of Physics and Technology
University of Bergen
Allegaten 55, 5007 Bergen
NORWAY
bjorn.kvamme@ift.uib.no

Abstract: - Production of natural gas from hydrate using carbon dioxide opens up for a win-win situation in which carbon dioxide can be safely stored in hydrate form while releasing natural gas from in situ hydrate. This concept has been verified experimentally and theoretically in different laboratories worldwide, and lately also through a pilot plant in Alaska. The use of carbon dioxide mixed with nitrogen has the advantage of higher gas permeability. Blocking of flow channels due to formation of new hydrate from injected gas will also be less compared to injection of pure carbon dioxide. The fastest mechanism for conversion involves the formation of a new hydrate from free pore water and the injected gas. As a consequence of the first and second laws of thermodynamics the most stable hydrate will form first in a dynamic situation, which involves that carbon dioxide will dominate the first hydrates formed from water and carbon dioxide / nitrogen mixtures. This selective formation process is further enhanced by favorable selective adsorption of carbon dioxide onto mineral surfaces as well as onto liquid water surfaces, which facilitates efficient heterogeneous hydrate nucleation. In this work we examine limitations of hydrate stability as function of gradually decreasing content of carbon dioxide. It is argued that if the flux of gas through the reservoir is high enough to prevent the gas from being depleted for carbon dioxide prior to subsequent supply of new gas, then combined carbon dioxide storage and natural gas production is still feasible. Otherwise the residual gas dominated by nitrogen will still dissociate the methane hydrate, if the released in situ CH4 from hydrate do not mix in with the gas but escape through separate flow channels by buoyancy. The ratio of nitrogen to carbon dioxide in such mixtures is therefore a sensitive balance between flow rates and rates for formation of new carbon dioxide dominated hydrate. Hydrate instability due to under saturations of hydrate formers have not been discussed in this work but might add additional instability aspects.

Key-Words: - methane hydrates, carbon dioxide storage, nitrogen, methane production

NOMENCLATURE

C Number of components in the Gibbs phase rule
E_P Potential energy [kJ/mol]
F Number of degrees of freedom in the Gibbs phase rule
F Free energy [kJ/mol]
f Free energy density [kJ/(mol m^3)]
f_i Fugacity [Pa]
g(r) Radial distribution function (RDF)
G Gibbs free energy [kJ/mol]
Δg_{kj}^{inc} Gibbs free energy of inclusion of Component k in cavity type j [kJ/mol]
H Enthalpy [kJ/mol]
h_{kj} Cavity partition function of Component k in cavity type j
k Cavity type index
K Ratio of mole-fraction gas versus mole-fraction liquid of the same component (gas/liquid K-values)
N_i Number of molecules
N Number of phases in the Gibbs phase rule
P Pressure [Pa]
P_0 Reference pressure [Pa]
r Distance [m]
R Molar gas constant [kJ/(K mol)]
T Temperature [K]
v_j No. of type j cavities per water molecule
v_m Molar volume [m^3/mol]
$\bar{V}_r$ Molar volume of *r*th component [m^3/mol]
$\bar{V}^{clath}$ Volume of clathrate [m^3]
x Mole fraction
y_w Mole fraction of water
Y Residual chemical potential per Kelvin

z Mole fraction
α Liquid (water) phase fraction
β Inverse of the gas constant times temperature
μ Chemical potential [kJ/mol]
$\mu_w^{0,H}$ Chemical potential for water in empty hydrate structure [kJ/mol]
θ_{kj} Fractional occupancy of cavity k by comp. j
γ Activity coefficient
ϕ Fugacity coefficient

1 Introduction

Injection of carbon dioxide into in situ natural gas hydrates in sediments will lead to conversion over to CO2 hydrate [1 - 3] and mixed CO2/CH4 hydrate [4 – 6], in which CO2 dominates filling of the large cavities. This is a win-win situation that ensures safe long time storage of CO2 while at the same time releasing CH4 for energy. There are two primary mechanisms that govern this conversion [4, 5]. Direct solid state conversion has been documented by various laboratories experimentally using NMR [7]. This is a very slow process limited by slow mass transport through hydrate. Another mechanism goes via formation of a new CO2 hydrate from injected CO2 and free water in the pores [4, 5]. The released heat from this formation will assist in dissociating the *in situ* CH4 hydrate. Adding N2 to the CO2 will reduce the thermodynamic driving force for the formation of new hydrate but some N2 will enter the hydrate although CO2 will dominate filling of the large cavities. Permeability increases proportional to N2 content. The added N2 will also reduce the risk for blocking the flow paths through the reservoir. Due to the combined first and second laws of thermodynamics the most stable hydrates will form first, which implies that CO2 will gradually be extracted for CO2 in a structure I hydrate, which easily facilitate hosting of CO2 in large cavity. Some CO2 might enter small cavity but the net stabilization of this small cavity filling is questionable. In a dynamic situation it is therefore likely that N2 will dominate small cavity filling. Another aspect that also facilitates CO2 dominance in hydrates, as long as there are significant CO2 amounts left in gas, is adsorption aspects. CO2 will adsorb well of different minerals, including Calcite [8, 9]. The selective adsorption onto liquid water can be examined by a simplified 2D adsorption theory [10 - 12]. As an example we now consider a gas of 90 mole% N2 and 10 mole % CO2.

$$(1)\quad \mu_i^{gas} = \frac{1}{\beta}\ln(\beta\Lambda_i^3) + \frac{1}{\beta}\ln(y_i\varphi_i^{gas}P)$$

where μ_i is chemical potential for component i, Λ_i is de Broglie wavelength for molecule i, β is the inverse of Boltzmann constant times temperature, ϕ_i is the fugacity coefficient for component i, P is pressure and y_i is the mole fraction of component i in the gas. The equilibrium between a gas molecule and same molecule adsorbed on the surface of liquid water may be expressed as:

$$\begin{aligned}
&\mu_i^{gass} = \frac{1}{\beta}\ln(\beta\Lambda_i^3) + \frac{1}{\beta}\ln(x_i N) \\
&-\frac{1}{\beta}\left(\frac{\partial \ln Q}{\partial N_i}\right)_{T,V,N_{j\neq i}} \\
&= \frac{1}{\beta}\ln(\beta\Lambda_i^3) + \frac{1}{\beta}\ln(x_i N) \\
&-\frac{1}{\beta}\left(\frac{\partial \ln Q^{2D}}{\partial N_i}\right)_{T,V,N_{j\neq i}} - \frac{1}{\beta}\ln Q_i^{1D} \\
&= \frac{1}{\beta}\ln(\beta\Lambda_i^3) + \frac{1}{\beta}\ln(x_i N) \\
&-\frac{1}{\beta}(\beta\mu_i^{2D}) - \frac{1}{\beta}\ln Q_i^{1D}
\end{aligned} \qquad (2)$$

in which the splitting into an orthonormal 2D plane assuming the horizontal structuring of the adsorbed layer does not affect the vertical interaction with the water surface. Q in equation (2) is the configurational part of the canonical partition function. The 1D part of the partition function in direction of the water as function of distance z from the surface is given by:

$$(3)\quad Q^{1D} \approx \int\left[\exp(-\beta\Gamma_{smooth}(z)) - 1\right]dz$$

In which $\Gamma_{smooth}(z)$ is the smoothed out distribution of water based on molecular dynamics simulation results [13] using TIP4P for water and simplified spherical Lennard-Jones 12-16 models for CO2 (Well-depth: 189.0 K and L-J diameter 3.615 Å) and N2 (Well-depth: 101.5 K and L-J diameter 4.486 Å). Lorentz-Berthelot mixing rules are applied. Soave-Redlich-Kwong [14] equation of state has been applied for gas phase. Further details on the 2D equation of state and other details of the adsorption

theory are given elsewhere [10 – 12]. At 30 bar and 273 K the estimated adsorption mole-fraction of CO2 is 32 mole per cent, i.e. roughly 3 times the mole-fraction of CO2 in the gas phase. Given this thermodynamic benefit of CO2 in the heterogeneous hydrate nucleation the question is how far down in CO2 concentration the depletion of CO2 from the gas can proceed before the gas is unable to create new hydrate. After this point then a second question arise. Will the *in situ* methane hydrate be stable towards this gas phase depleted of CO2 or will it dissociate? Then yet a third question will arise. Will the formed CO2 dominated hydrate remain stable in an environment of CH4/N2 dominated gas phase? The paper is organized as follows. The thermodynamic models are given in section 2 followed by a section for verification of the models in section 3 and a more detailed analysis and discussion of stability limits in section 4. Our conclusions are given in section 5.

2 Theory

2.1 Fluid Thermodynamics

Formally, a thermodynamic equilibrium is achieved when the temperatures, pressures and chemical potentials of all co existing phases are uniform across all phase boundaries. To insure the same reference values for free energy of all phases, the calculation of chemical potentials of all components in the different phases should use ideal gas as the reference state:

$$\mu_i(T,P,\vec{y}) - \mu_i^{ideal\,gas}(T,P,\vec{y}) = RT\ln\phi_i(T,P,\vec{y}) \quad (4)$$

where ϕ_i is the fugacity coefficient for component *i* in a given phase.

As an intermediate step, another reference state for the chemical potential of a liquid state component *i* will also be used:

$$\mu_i(T,P,\vec{x}) - \mu_i^{idealliquid}(T,P,\vec{x}) = RT\ln\gamma_i(T,P,\vec{x}) \quad (5)$$

$$\lim(\gamma_i) = 1.0 \quad \text{when } x_i \to 1.0$$

where γ_i is the activity coefficient for component i in the liquid mixture. Note that equation (3) as applied to water is also based on absolute thermodynamics when chemical potential of pure water is calculated from models using molecular simulations. More specifically, we will use data from Kvamme & Tanaka [15].

Yet another reference state will prove useful in case of gases with low solubility in water:

$$\mu_i(T,P,\vec{x}) - \mu_i^{\infty}(T,P,\vec{x}) = RT\ln\left[x_i\gamma_i^{\infty}(T,P,\vec{x})\right] \quad (6)$$

$$\lim(\gamma_i^{\infty}) = 1.0 \quad \text{when } x_i \to 0$$

where the ∞-superscript stands for the infinite dilution. This particular convention is known as the non-symmetric convention since the limit of the activity coefficient for the component *i* will approach unity as its the mole fraction vanishes. One way to estimate absolute values for these infinite dilution chemical potentials is through molecular dynamics simulations and the application of the Gibbs-Duhem relation [16, 17].

Provided that thermodynamic properties of all phases can also be specified and evaluated outside of the equilibrium, the first and second laws of thermodynamics would require that the available mass of each component, and the total mass, should be distributed over all possible phases able to coexist under given local pressure and temperature conditions. This evaluation will be fairly straightforward for most of the fluid phases under consideration. The only phase requiring a special attention will be the hydrate phase, which is discussed extensively in Kvamme *et al* [18]. Combining thermodynamic formulations for fluids in equations (4) to (6) with hydrate non-equilibrium formulations from Kvamme *et al* [18] makes it fairly straightforward to minimize the free energy and obtain estimates for local phase distributions obeying the first and the second law of thermodynamics. Several algorithms capable of implementing this approach are available in the open literature.

Situations considered here imply very limited solubility and/or limited concentrations. The solubility of H_2O in CO_2/N2 is very low. In view of this fact, the following approximation should prove sufficiently accurate for pure liquid CO_2 (or CO2 with small amounts of N2 but still in liquid) limit:

$$\mu_{i,j}(T,P,\vec{x}) \approx \mu_{i,j}^{\infty}(T,P) + RT\ln\left[x_{i,j}\gamma_{i,j}^{\infty}(T,P,\vec{x})\right] \quad (7)$$

where subscript *j* refers to components; subscript *i* denotes the phase. In the context of this work, *j* is

"CO_2" in case of the CO_2 phase, and "H_2O" for the aqueous phase, "ads" refers to the phase adsorbed on hematite, and "H" is the solid hydrate phase. For water dissolved in gas mixtures of CO2 and N2 the solubility is low enough to approximately cancel the water/water term in the attractive parameter so at the cost of some rigor rough estimates of liquid water drop-out can also be achieved [6].

2.2 Equilibrium thermodynamics of hydrate

Applying the statistical mechanical model for water in hydrate [15] yields the following equation for chemical potential of water in hydrate:

$$(8)\quad \mu_w^{O,H} - \sum_{k=1,2} RTv_k \ln\left(1+\sum_i h_{ik}\right)$$

where subscript H denotes the hydrate phase, superscript 0 stands for the empty hydrate, v_k is the fraction of cavity of type k per water. For structure I hydrate, v_k = 1/23 for small cavities (20 water molecules) and 3/23 for large cavities (24 water molecules). h_{ik} is the canonical partition function for a cavity of type *k* containing a "quest" molecule of type *i*; it is given by:

$$(9)\quad h_{ik} = e^{\beta\left(\mu_i^H - \Delta g_{ik}^{inc}\right)}$$

where β is the inverse of the gas constant times temperature while Δg_{jk}^{inc} reflects the impact on hydrate water from the inclusion of the "guest" molecule *i* in the cavity [15]. At equilibrium, chemical potential μ_i^H has to be identical to chemical potential of molecule *i* in the phase it has been extracted from. The hydrate content of all gas components can be estimated by applying equation (4) to calculate their chemical potential when dissolved in the methane phase. Water will totally dominate the dew point. So a simple approximation for hydrate formation in case of liquid water drop-outcan be obtained by applying equation (10) below.

$$\begin{aligned}(10)\quad &\mu_w^{O,H} - \sum_{k=1,2} RTv_k \ln\left(1+\sum_i h_{ik}\right)\\ &= \mu_{i,H2O}^{purewater}(T,P)\\ &+RT\ln\left[x_{i,H2O}\gamma_{i,H2O}(T,P,\vec{x})\right]\end{aligned}$$

Note that chemical potential of the empty hydrate structure estimated basing on Kvamme & Tanaka [15] has been verified to have predictive capabilities, which makes any empirical formulations redundant and maybe unphysical since chemical potential is a fundamental property. Throughout this study we approximate the right hand side of (10) by pure water. This will imply a limited shift to the chemical potential of liquid water. As an example the correction at 150 bar and 274 K will be -0.07 kJ/mole and slightly higher for 200 bars and 250 bars but still not dramatic for the purpose of this study.

$$(11)\quad G^H = \sum_i x_i^H \mu_i^H$$

The non-equilibrium description of hydrate due to Kvamme *et al* [2] can be applied for this purpose to follow free energy gradients until the CO2/N2 phase has been mostly depleted in the most aggressive hydrate former, carbon dioxide. The analysis of equation (9) will also require the knowledge of hydrate composition; it can be found by applying statistical thermodynamic theory to the adsorption model for hydrate (left hand side of equation (10)); the composition will be given by:

$$(12)\quad \theta_{ik} = \frac{x_{ik}^H}{v_k\left(1-x_T\right)} = \frac{h_{ik}}{1+\sum_i h_{ik}}$$

where θ_{ik} is the filling fraction of component in cavity type k, x_{ik}^H is the mole fraction of component i in cavity type k, x_T is the total mole fraction of all guests in the hydrate, and v_k is, as defined above, the fraction of cavities per water of type k.

Computed free energies of quest inclusion in the large cavity of structure I have been fitted to a series in inverse reduced temperature.

$$(13)\quad \Delta g^{inclusion} = \sum_{i=0}^{5} k_0 \left[\frac{T_c}{T}\right]^i$$

where T_c is the critical temperature of the guest molecule in question (see tables 1, 2 and 3). There is some different experimental evidence that CO2 also enters the small cavity but during our MD studies we don't find that it gives any net stabilizing effect of the hydrate. For most CO2 models we have tested the hydrate structure collapses. It does not mean that

CO2 will not be able to be "forced" into the small cavities but it still remain unverified if this would happen in dynamic flow situations to any significant extent. So as far as practical hydrate predictions related to flow problems and corresponding dynamic situations it is not obvious that possible inclusion in small cavities needs to be included since the cavity partition function for CO2 in small cavity (equation (9)) might be close to zero anyway.

k	Large cavity	Small cavity
0	14.631108552734160	0
1	-0.4714182199600883	0
2	-91.773951637448920	0
3	2.249867200986224	0
4	11.027927839813380	0
5	19.622948066966590	0

Table 1: Coeffcient of $\Delta g^{inclusion}$ in case of carbon dioxide inclusion. Critical temperature for CO_2 is 304.13 K. At present stage it is assumed that no CO2 enters the small cavity and correspondingly the 0 for small cavity.

k	Large cavity	Small cavity
0	15.953190676883240	-39.0604373928416
1	-13.349289598714340	121.665319263939
2	-166.526506256734500	185.436683224177
3	28.068892414980430	116.575797703473
4	41.945206442433370	-54.393598344663
5	151.1540705347040	-82.9143384357272

Table 2: Coeffcient of $\Delta g^{inclusion}$ in case of CH4 inclusion. Critical temperature for CH_4 is 190.56 K.

The free energy of inclusion in equation (7) can be estimated according to Kvamme & Tanaka [15. Thermodynamic consistency has been a high priority throughout this work, and it was not our intention to adjust any parameters to fit experimental data. Molecular dynamics simulations reported in this work were restricted to extending the approach of [15] to larger hydrate systems and additional temperatures between 273.16 K and 280 K, which is the temperature range in this study.

k	Large cavity	Small cavity
0	-45.55039046631593	-199.1824874694727
1	18.545729464463110	266.23940583971190
2	-131.7881893149816	8.448543642023667
3	103.0832372020720	352.2548526908923
4	27.759086907720460	-10.844174184315280
5	141.643579069865200	-60.103750139641910

Table 3: Coeffcient of $\Delta g^{inclusion}$ in case of nitrogen inclusion. Critical temperature for N_4 is 126.19 K.

Updated parameters for free energy of inclusion are given in tables 1 to 3. Parameters for empty hydrates and ice were not significantly affected and the parameters of Kvamme & Tanaka [15] were applied. Similarly, the estimates for the chemical potential of liquid water were extended from 0 Celsius by means of thermodynamic relationships and experimental data on enthalpy of dissociation and liquid water heat capacities. See Kvamme & Tanaka [15] for more details.

3. Results and discussion

It is not our intension to present a quantitative and fitted model for the CO2/N2 hydrate/fluid system. Rather than tuning the model towards experimental data we prefer to keep the simulated [15] properties of the hydrate and a fairly simple equation of state. Our range of interests for gas mixture systems keep us in the gas range so SRK equation of state [14] is deemed accurate enough for our purpose.

3.1 Verification of the model

It should be noted that all results in figures 1 to 5 below have been estimated without accounting for Poynting corrections to liquid water and empty clathrate in equation (10). For the ranges of pressures in figures 1 to 5, as well as for the ranges of pressures in this study the Poynting corrections on left and right hand side of (10) would imply the pressure integral of difference in molar volumes of liquid water and empty clathrate water which practically has negligible impact. We should keep in mind that the CO2 ideal gas properties are calculated from a non-spherical model [6, 8]. We are not aiming at empirical fitting of parameters to achieve quantitative agreement in this work. Within the focus of this paper the model systems are deemed accurate enough.

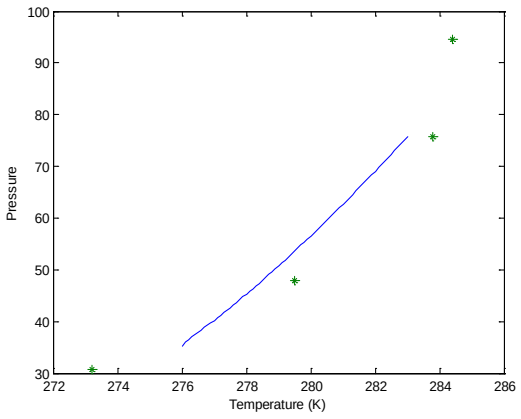

Fig. 1. Estimated equilibrium curve for a system of 50% CO2 and 50% N2 (solid line) versus experimental data from [19] (*).

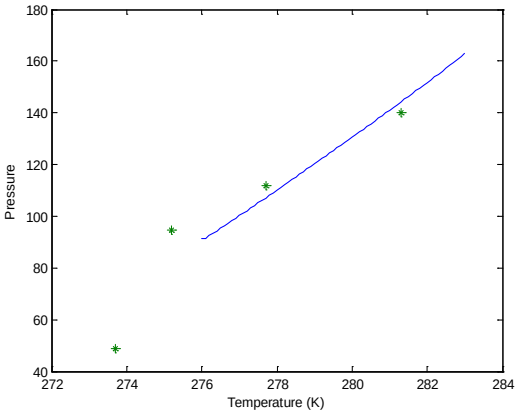

Fig. 2. Estimated equilibrium curve for a system of 10% CO2 and 90% N2 (solid line) versus experimental data from [18] (*).

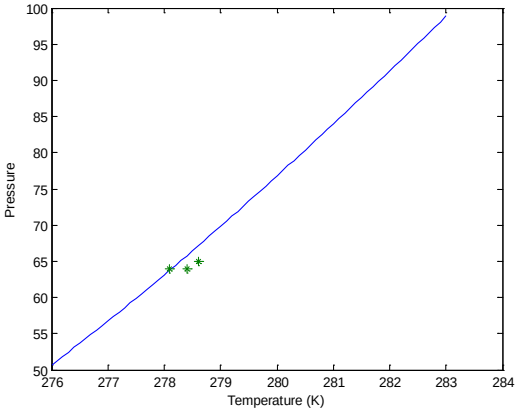

Fig. 3. Estimated equilibrium curve for a system of 30% CO2 and 70% N2 (solid line) versus experimental data from Herri *et.al.* [19] (*).

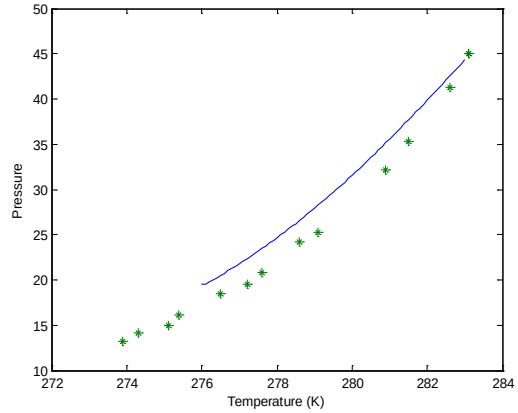

Fig. 4. Estimated equilibrium curve for pure CO2 hydrate equilibrium (solid line) versus experimental data from Herri *et.al.* [19] (*).

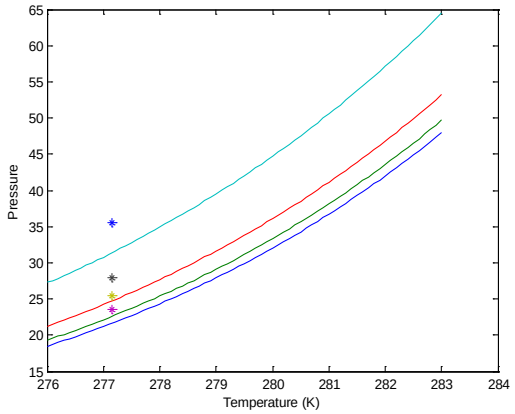

Fig. 5. Estimated equilibrium curves (solid) for CO2 with different contents of CH4. From bottom: 64 mole % CO2. 52 mole % CO2, 36 mole % and 11 mole %. Experimental data from Herri *et.al.* [19] (*) in same order as for the estimated curves.

3.2 Limits of hydrate stability for mixtures of CO2 and N2.

Equilibrium curves as estimated for different CO2 mole-fractions in nitrogen are plotted in figure 6. Estimated water chemical potentials in hydrate and liquid water for pressures of 100, 150, 200 and 250 bars are plotted in figures 7 to 10 under approximations that guest chemical potentials are same in hydrate and gas but no water equilibrium. For 100 bars hydrate is not stable for mole-fraction of CO2 less than 20 mole % at 280 K. As expected this region of instability is reduced as pressure increases, as seen from figures 8 to 10. Pressures as low as 50 bars may not be relevant for production of hydrate but a similar plot of estimated chemical potentials for 50 bars is given in figure 11. At this low pressure hydrates of less than 60 mole % CO2 is not stable at 280 K.

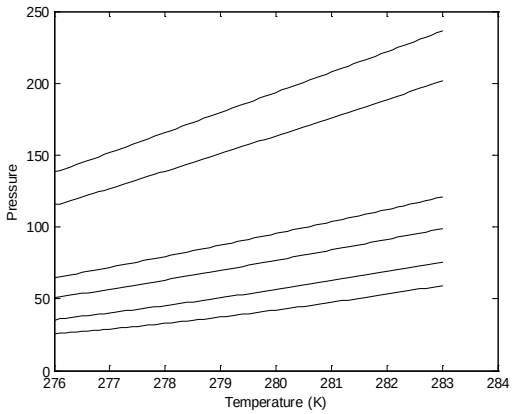

Fig. 6. Estimated equilibrium curves (solid) for CO2 with different contents of N2. From bottom: 75 mole % CO2.

50 mole % CO2, 30 mole % CO2, 20 mole % CO2 , 10 mole % CO2 , 5 mole % CO2 and 2 mole % CO2.

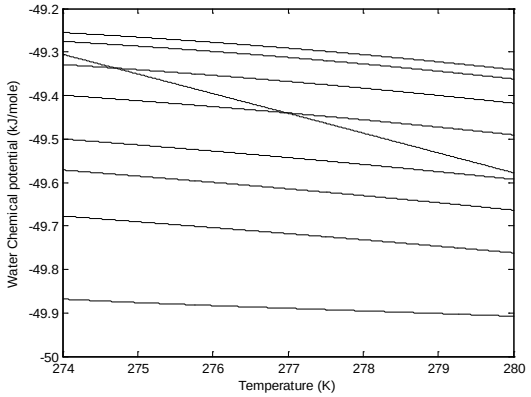

Fig.7. Estimated water chemical potential in hydrate (solid) and liquid water (dash) as function of temperature for 100 bars and CO2 mole-fractions of 0.75, 0.5, 0.3, 0.2, 0.1, 0.05, 0.02, 0.01, with 0.75 mole-fraction curve lowest and 0.01 mole-fraction curve on top.

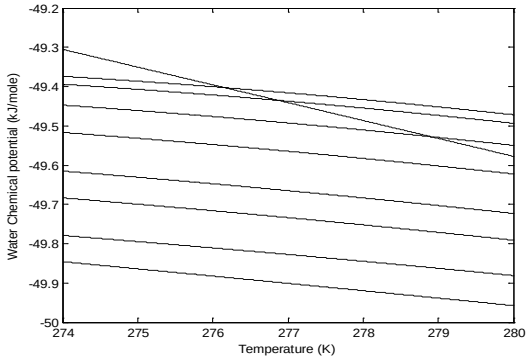

Fig.8. Estimated water chemical potential in hydrate (solid) and liquid water (dash) as function of temperature for 150 bars and CO2 mole-fractions of 0.75, 0.5, 0.3, 0.2, 0.1, 0.05, 0.02, 0.01, with 0.75 mole-fraction curve lowest and 0.01 mole-fraction curve on top.

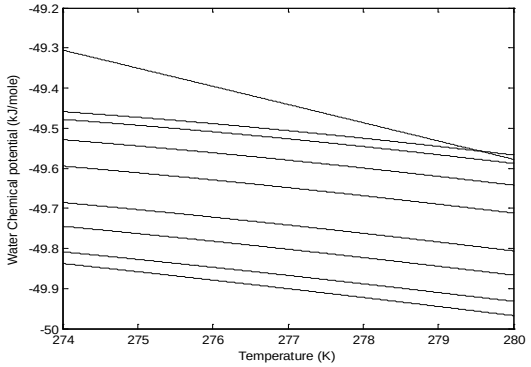

Fig.9. Estimated water chemical potential in hydrate (solid) and liquid water (dash) as function of temperature for 200 bars and CO2 mole-fractions of 0.75, 0.5, 0.3, 0.2, 0.1, 0.05, 0.02, 0.01, with 0.75 mole-fraction curve lowest and 0.01 mole-fraction curve on top.

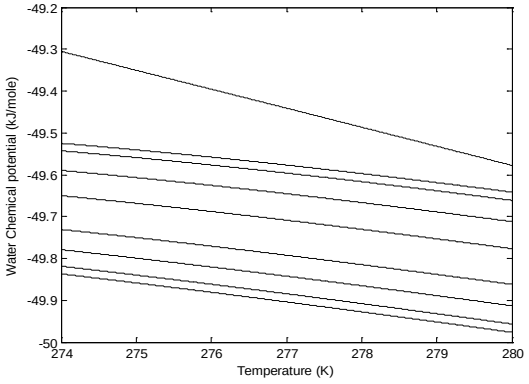

Fig.10. Estimated water chemical potential in hydrate (solid) and liquid water (dash) as function of temperature for 250 bars and CO2 mole-fractions of 0.75, 0.5, 0.3, 0.2, 0.1, 0.05, 0.02, 0.01, with 0.75 mole-fraction curve lowest and 0.01 mole-fraction curve on top.

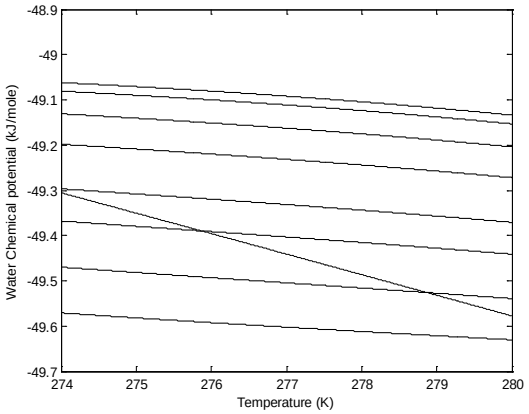

Fig.11. Estimated water chemical potential in hydrate (solid) and liquid water (dash) as function of temperature for 50 bars and CO2 mole-fractions of 0.75, 0.5, 0.3, 0.2, 0.1, 0.05, 0.02, 0.01, with 0.75 mole-fraction curve lowest and 0.01 mole-fraction curve on top.

3.2 Limits of hydrate stability for mixtures of CO2, N2 and CH4.

After the exchange have started the mixture of CO2 and N2 will get diluted with released CH4. Within the limited space of this paper we therefore investigate stability limits for two gas mixtures. Mixture 1 has 25 mole % CH4 and the remaining 75 mole % is distributed between CO2 and N2 as in the cases studied in section 3.1. The corresponding mole-fractions of CO2 are thus: 0.563, 0.375, 0.225, 0.15, 0.075, 0.0375, 0.015 and 0.0075. Mixture 2 has 50 mole % CH4 and the remaining 50 mole % is distributed between CO2 and N2 as in the cases

studied in section 3.1. The corresponding mole-fractions of CO2 are thus: 0.375, 0.25, 0.15, 0.10, 0.05, 0.025, 0.01 and 0.005.

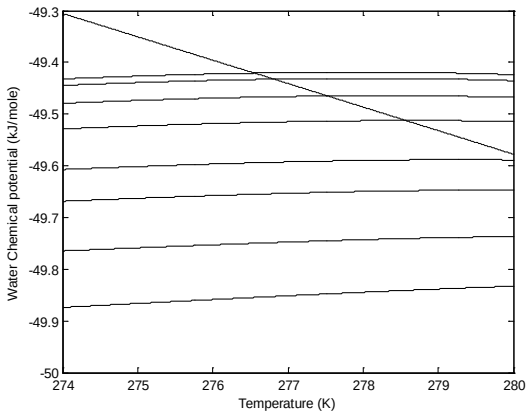

Fig.12. Estimated water chemical potential in hydrate (solid) and liquid water (dash) as function of temperature for 75 bars for mixture 1. Lowest curve is for highest CO2 content.

3.3 Gas phase under saturated by CH4

As observed from the results in section 3.2 CH4 will assist construction of new mixed hydrate if CH4 mixes in with the CO2/N2 mixture. If, however, the heat generated dissociation of the *in situ* CH4 hydrate leads to CH4 disappearing through other pathways which do not lead to mixing with the inflowing gas then the chemical potential difference between CH4 in the clathrate will be higher than what would be chemical potential for CH4 in the gas at infinite dilution. This is illustrated in figure 16 which is estimated for 1% CH4 in two CO2/N2 mixtures.

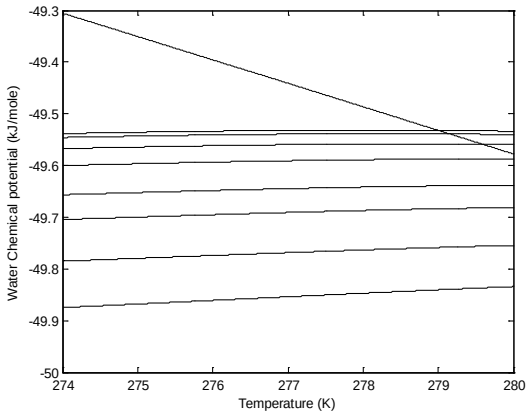

Fig.13. Estimated water chemical potential in hydrate (solid) and liquid water (dash) as function of temperature for 75 bars for mixture 2. Lowest curve is for highest CO2 content.

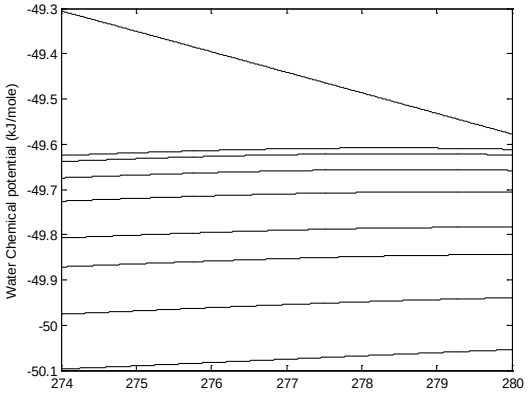

Fig.14. Estimated water chemical potential in hydrate (solid) and liquid water (dash) as function of temperature for 130 bars for mixture 1. Lowest curve is for highest CO2 content

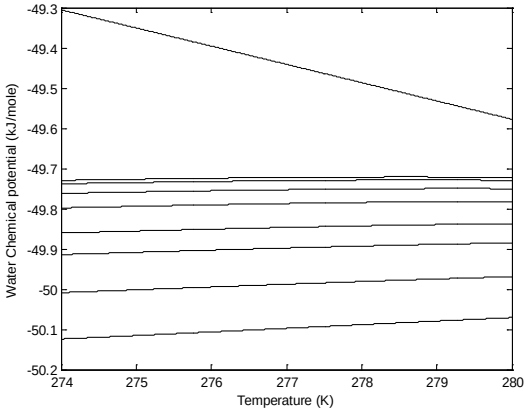

Fig.15. Estimated water chemical potential in hydrate (solid) and liquid water (dash) as function of temperature for 130 bars for mixture 2. Lowest curve is for highest CO2 content

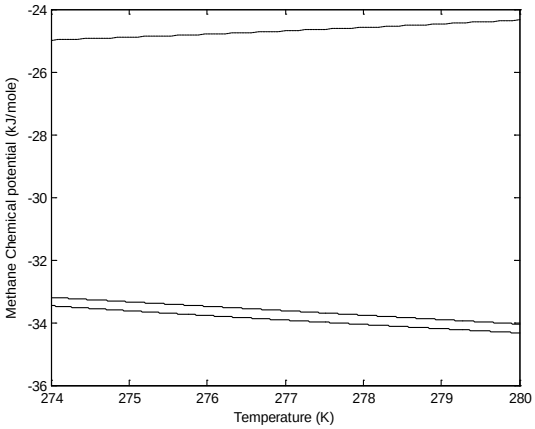

Fig. 16. Estimated chemical potential for CH4 in equilibrium hydrate (--) versus chemical potential for 1% CH4 in gas of 1% CO2 in N2 (top solid line) at 100 bar pressure and 1% CH4 in 75% CO2 in N2 (bottom solid line) at 100 bar pressure.

The minimum pressure on the CH4 equilibrium chemical potentials in 35.7 bar at 274 K and the maximum pressure is 62.7 bar at 280 K. The values of the dashed curve should therefore have been slightly higher due to a Poynting correction from actual P to 100 bars, which implies very minor corrections [5, 6]. And strictly speaking also a sub saturation effect in filling fractions for the higher pressures, which is also negligible [5, 6].

In situ CH4 hydrate will therefore dissociate towards gas due to chemical potential gradients of CH4. The 75% CO2 curve in 16 is just plotted in order to illustrate that 1% CH4 in gas is limited sensitive to CO2/N2 ratio at this pressure and the limited range in temperature.

3.4 Chemical potential gradients for CO2 between gas and hydrate.

Similar to section 3.3 we can also evaluate gradients in chemical potential for CO2 in a pure CO2 hydrate and compare to chemical potentials for CO2 in CO2/N2 gas mixtures. From figure 17 below it is observed that a pure CO2 hydrate will only dissociate in chemical potential gradient of CO2 if the mole-fraction of CO2 in the gas mixture is less than 50 mole % (for 280 K). In figure 7 under section 3.1 no equilibrium criteria for water is assumed but hydrate guest chemical potentials are assumed to be the same in gas and hydrate. There is a slight shift if the hydrate is initially made from a gas mixture of 75% CO2 and rest N2. At 100 bar this mixed hydrate can remain stable towards CO2 in gas down around 42 mole% CO2.

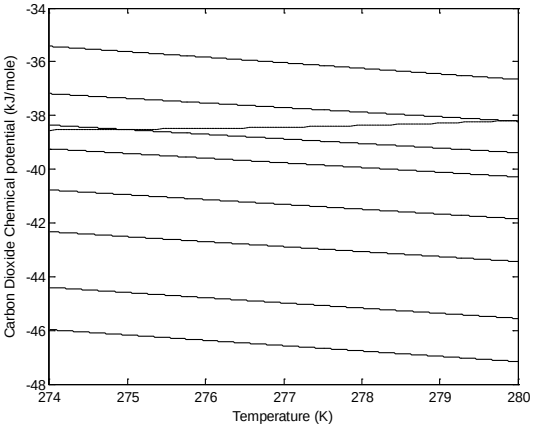

Fig. 17. Estimated chemical potential for CO2 in pure CO2 equilibrium hydrate (--) versus chemical potential for CO2 in gas mixtures with CO2 mole-fractions (from top): 0.75, 0.50, 0.30, 0.20, 0.10, 0.05, 0.02, 0.01, all at 100 bars. Equilibrium pressures range from 25.3 bars at 274 K to 41.6 K at 280 K.

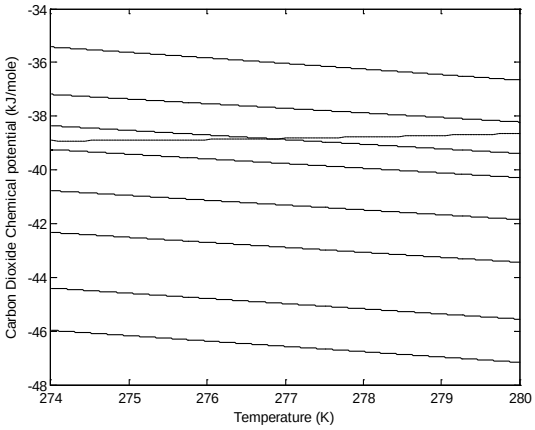

Fig. 18. Estimated chemical potential for CO2 in hydrate from 75 mole % CO2 and 25 mole % N2 at equilibrium hydrate (--) versus chemical potential for CO2 in gas mixtures with CO2 mole-fractions (from top): 0.75, 0.50, 0.30, 0.20, 0.10, 0.05, 0.02, 0.01, all at 100 bars. Equilibrium pressures range from 25.3 bars at 274 K to 41.6 K at 280 K.

4. Conclusions

The fastest mechanism for exchange between *in situ* CH4 hydrate and injected CO2/N2 mixtures is through formation of a new hydrate. In this work we have examined hydrate formed from different mixtures of CO2, N2 and CH4 under the assumption that gas phase chemical potentials is the same in hydrate but with no equilibrium constraints on water so that it is possible to examine differences in chemical potential for water in hydrate with liquid water chemical potential in terms of stability limits. For pressures as low as 50 bar this require approximately 60% CO2 in the gas mixture while at 100 bar the number is 20% under these approximations. For high pressures new hydrate formation is possible for hydrate formed from substantially lower amount of CO2 in the gas phase. CO2 will benefit from selective adsorption onto mineral surfaces as well as onto liquid water. This, in combination with implication of first and second laws of thermodynamics, will lead to a gradual extraction of CO2 from the gas phase. If the pressure is as high as 250 bars for the range of temperatures 274 to 280 K then new hydrate can form down to very low fractions of CO2. If the flux of CO2 depletion from the injected gas phase is higher than the flow rate flux between an injection well and a producing well then new hydrate formation will depend on how much of the released CH4 than can assist in creating a new mixed hydrate from CO2, CH4 and N2. If CH4 for some reason (like for instance finding it's pathways of escape by buoyancy) do not participate in new hydrate formation then the hydrate will have a driving force

to dissociate towards a gas phase which is under saturated with methane. Instability aspects due to hydrate guest molecules which are under saturated with reference tp pure water (as used in this study) have not been discussed here but will be devoted attention in follow up studies. Some indications on this aspect can be found elsewhere [20, 21].

References

[1] Kvamme, B, Graue, A., Kuznetsova, T., Buanes, T., Ersland, G., *Storage of CO2 in natural gas hydrate reservoirs and the effect of hydrate as an extra sealing in cold aquifers*, International Journal of Greenhouse Gas Control, 2007, Vol ½, 236-246

[2] Kvamme, B, Graue, A., Kuznetsova, T., Buanes, T., Ersland, G., *Exploitation of natural gas hydrate reservoirs combined with long term storage of CO2*, WSEAS TRANSACTIONS on Environment and Development, 2006, 2(6), 699 - 710

[3] György Tegze, László Gránásy, Bjørn Kvamme, *Theoretical modeling of the conversion of methane hydrate into carbon dioxide hydrate*, PCCP, 2007, 9, 3104 – 3111

[4] Khuram Baig, Bjørn kvamme, Tatiana Kuznetsova, Jordan Bauman, *The impact of water/hydrate film thickness on the kinetic rate of mixed hydrate formation during CO2 injection into CH4 hydrate*, 2014, submitted to AIChE journal

[5] Bjørn Kvamme, Muhammad Qasim, Khuram Baig, Pilvi-Helinä Kivelä, Jordan Bauman, *Phase field theory modeling of methane fluxes from exposed natural gas hydrate reservoirs*, International Journal of Greenhouse Gas Control, 2014, 29, 263–278

[6] Bjørn Kvamme, Tatiana Kuznetsova, Pilvi-Helina Kivelæ and Jordan Bauman, *Can hydrate form in carbon dioxide from dissolved water?*, 2013, PCCP, 15 (6), 2063 - 2074.

[7] Huen Lee, Yongwon Seo, Yu-Taek Seo, Igor L. Moudrakovski, John A. Ripmeester, *Recovering Methane from Solid Methane Hydrate with Carbon Dioxide*, Angewandte Chemie International Edition, 2003, Volume 115 Issue 41 Pages 5202 – 5205

[8] Van Cuong, P. Kvamme, B. Tatiana Kuznetsova, T., Jensen, B., *The Impact of Short-Range Force Field Parameters and Temperature Effect On Selective Adsorption of Water and CO2 On Calcite*, International Journal of Energy and Environment, 2012, Volume 6, 301-309

[9] Van Cuong, P., Kvamme, B. Kuznetsova, T., Jensen, B., *Molecular dynamics study of calcite and temperature effect on CO2 transport and adsorption stability in geological formations*, Molecular Physics, 2012, Volume 110, Issue 11-12, 1097-1106

[10] Vuong, T. , and Monson, P. A., Langmuir, 1996, 12, 5425.

[11] Shen, J., and Monson, P. A., Molec. Phys., 2002, 100, 2031

[12] Kierlik, E., Monson, P. A., Rosinberg, M. L., and Tarjus, G., J. Chem. Phys., 1995, 103, 4256.

[13] Kvamme, B., *Thermodynamic Properties and Dielectric Constants in Water-Methanol Mixtures by Integral Equation Theory and Molecular Dynamics Simulations*. Physical Chemistry Chemical Physics 2002; 4:942-948

[14] Soave G. *Equilibrium constants from a modified Redlich-Kwong equation of state*. Chem. Eng. Sci. 1971; 27: 1197-1203.

[15] Kvamme B, Tanaka H. *Thermodynamic Stability of Hydrates for Ethane, Ethylene, and Carbon Dioxide* J PhysChem 1995; 99: 7114-7119.

[16] Kvamme, B., Kuznetsova, T., Jensen, B., Stensholt, S., Sjøblom, S. and Lervik, K.N., *Investigating chemical potential of water and H2S dissolved into CO2 using molecular dynamics simulations and Gibbs-Duhem relation*, 2014, submitted to Fluid Phase Equilibria

[17] Kvamme, B., Kuznetsova, T., Jensen, B., Stensholt, S., Bauman, J., Sjøblom, S. and Nes Lervik, K., *Consequences of CO2 solubility for hydrate formation from carbon dioxide containing water and other impurities*, *Phys. Chem. Chem. Phys.*, 2014, 16 (18), 8623 – 8638

[18] Bouchafaa, W., Dalmazzone, D., *Thermodynamic equilibrium data for mixed hydrates of co2-n2 , co2-ch4 and co2-h2 in pure water and TBAB solutions*, Proceedings of the 7th International Conference on Gas Hydrates, Edinburgh, Scotland, United Kingdom, July 17-21, 2011

[19] Herri, J.-M. Bouchemoua, A., Kwaterski, M. Fezoua, A., Ouabbas, Y., Cameirao, A., *Gas hydrate equilibria for CO2–N2 and CO2–CH4 gas mixtures—Experimental studies and thermodynamic modelling*, Fluid Phase Equilibria, 2011, 301, 171–190

[20] Kvamme, B, *Kinetics of Hydrate Formation from Nucleation Theory*, *Int. J. Offshore Polar Eng.*, 2002, 12(4), 256-263

[21] Kvamme, B., *Droplets of Dry Ice and Cold Liquid CO_2 for Self-Transport of CO_2 to Large Depths*, *Int. J. Offshore Polar Eng.*, 2003, 13(2), 139-146